SIMULATION AND OPTIMIZATION OF TRANSPORT IN A LINEAR BROWNIAN MOTOR

B.C. Trzynadlowski[1], S. Volz[2], S.T. Dunham[1], E. Altintas[2], H. Fujita[2], and K.F. Böhringer[1]*
[1]University of Washington, Seattle, WA, USA
[2]University of Tokyo, Tokyo, JAPAN

ABSTRACT

Linear Brownian motors utilize relatively weak electric fields to bias the diffusion of particles in a microfluidic channel thereby harnessing Brownian motion to facilitate particle transport. We present a custom simulator for such a system and use it to optimize transport by modifying the electrode configuration and rectification scheme. With insight gained from simulation, we are able to identify features of potential energy profiles conducive to faster transport and suggest configurations to achieve them.

KEYWORDS

Brownian motor, nanoscale transport, dielectrophoresis, simulation.

INTRODUCTION

Brownian ratchet mechanisms described in the literature [1] often rely on an asymmetrical potential to bias the diffusion of particles. In our system, it is the switching sequence itself that provides the bias; the potential is symmetric. Fig. 1 is a schematic illustration of the motor. Nanobeads in a microfluidic channel are subjected to dielectrophoretic (DEP) forces imparted by electrodes implanted below the channel. By gradually moving this potential along in a given direction, particles diffusing in the same direction as the motion of the potential wells tend to be nudged along, thus biasing the motion in a particular direction. The electric fields are relatively weak, and serve to bias the Brownian motion of the particles in a particular direction.

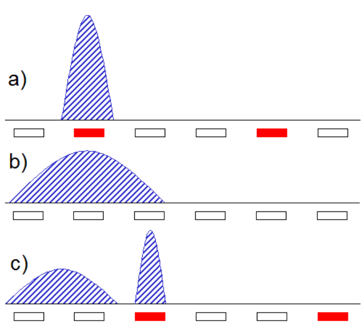

Figure 1: Three-phase rectification. a) The population of particles is attracted to the activated electrodes during the ON time. b) The particles diffuse freely during the OFF time. c) The next set of electrodes is activated.

A three-phase rectification scheme is used whereby every third electrode is activated for a length of time (the ON time) and then switched off (OFF time) before beginning the next cycle [2]. It was suggested in [3] that the addition of a ground plane above the channel would produce stronger confinement and increase transport velocity. In this paper, we examine such a modification, as well as the effect of rectification scheme, and comment on how this enhances transport.

MODELING

Transport in the simulator is modeled with a large ensemble of independent particles, each governed by the Langevin equation [4],

$$m\frac{d^2x}{dt^2} = -\gamma\frac{dx}{dt} + \sqrt{2\cdot\gamma\cdot k_B\cdot T}\,\xi(t) + F_{DEP}(x,t) \qquad (1)$$

This equation includes a viscous term, defined by Stokes' law,

$$\gamma = 6\pi\cdot\upsilon\cdot a \qquad (2)$$

where *a* is the particle radius and   is the viscosity of the suspending fluid. Normally-distributed Gaussian white noise, *(t)*, scaled by a term related to the thermal energy of the fluid is used to model Brownian motion. The external DEP force term, F_{DEP}, is dependent on the electric field and therefore the electrode configuration. For a particle of radius *a*, the DEP force is given as

$$F_{DEP} = 2\pi a^3\varepsilon_m \mathrm{Re}\{f_{CM}\}\nabla|E_{rms}|^2 \qquad (3)$$

where ε_m is the permittivity of the medium, f_{CM} is the Clausius-Mossotti factor (taken to be 1.0 as in [2]), and E_{rms} is the electric field as calculated from the RMS value of the electrode voltage [5,6].

The DEP force along the direction of the channel due to an active electrode (0.25 V_{RMS}) is obtained from an electrostatic calculation [1,3] performed using COMSOL Multiphysics. The force profile is sampled at different heights in the channel, necessary because the particles are large compared to channel height. The overall DEP force is computed by taking a weighted average, based on particle surface area.

There is no closed-form solution to (1) because (3) is sampled from simulation data. A simple approximation, assuming that particle velocities are relatively low and the variation in the potential profile is gradual, is to solve (1) taking the total applied force, F (Brownian and DEP terms), as constant during each time step; the result is (4), where v_0 and x_0 are the initial velocity and position.

$$x(t) = \frac{m}{\gamma}\left(v_0 - \frac{F}{\gamma}\right)\left(1 - \exp\left\{-\frac{\gamma}{m}t\right\}\right) + \frac{F}{\gamma}t + x_0 \qquad (4)$$

The relaxation time can be approximated as m/γ, which is on the order of nanoseconds, impractically small for simulation purposes. Practical time steps, on the order of 10^{-5} to 10^{-3} seconds, are sufficiently long to allow inertial effects to be ignored, leading to a simple and computationally efficient quasi-static solution,

$$x(t) = \frac{F_{DEP} + \sqrt{2 \cdot \gamma \cdot k_B \cdot T}\xi}{\gamma}t + x_0 \qquad (5)$$

Although written in 1D form here, the simulator generalizes this approach to two dimensions: channel length (x-axis), and height (y-axis.) Bilinear interpolation is used to sample the DEP force at any given point in the channel.

RESULTS

Ground Plane Configuration

Our simulator framework takes electric field data directly from electrostatic simulations in order to compute the DEP force exerted on a particle. We assume that grounded electrodes flanking active ones will terminate the electric field lines, allowing us to investigate larger-phase rectification schemes by assuming the force is negligible between pairs of inactive electrodes (as seen in Fig. 2).

We investigate a configuration similar to the one proposed in [2], but with a 2 µm-deep channel, with different ground plane configurations. Fig. 2 is a visualization of one of the configurations as simulated in COMSOL. Fig. 3 shows the potential experienced by a particle at the bottom of the channel for each of the configurations: no ground plane, ground plane 2 µm above the channel floor, and ground plane 6 µm above. In each case we examine the effect of different rectification schemes (effectively increasing the distance between active electrodes) on net average transport velocity. For purposes of comparison, the OFF time is kept at 0 seconds and the ON time is varied. The number of cycles over the N electrodes (3, 4, or 5) in the rectification scheme is fixed at 5 [7], therefore the simulation time varies with ON time as $5 \times N \times T_{ON}$. Figs. 4-6 show the effect of ON time and rectification scheme on average velocity. All simulations were conducted at a temperature of 298.15 K. Average velocity is computed by dividing the net displacement of each particle by the simulation time.

Without a ground plane, the coupling between active and neighboring inactive electrodes produces a wide potential with multiple local minima. During each cycle, this potential profile moves forward by 6 µm (the center-to-center electrode spacing.) A particle initially confined to one of the minima in the right half of the well will find itself in the left half of the potential well on the next cycle, confined again in roughly the same location it started. A particle initially confined in the left half of the well will find itself in a region between adjacent wells without strong DEP forces, assuming three-phase rectification where the potential profiles of Fig. 3 are periodic over 18 µm. Brownian motion is equally likely to carry this particle towards either well. Therefore, particles are somewhat more likely to be caught in the forward-moving wells than to fall behind.

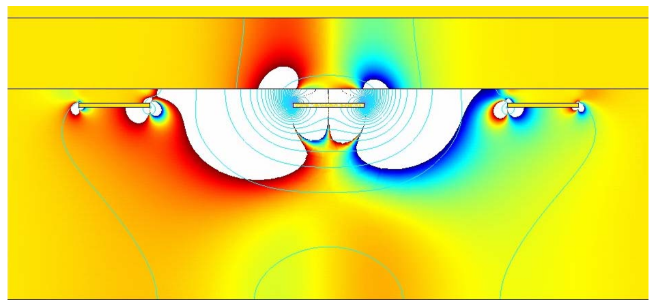

Figure 2: COMSOL visualization of 2 µm-channel structure. Here, a ground plane is present just above the channel. Contours represent the gradient of the square of the electric field.

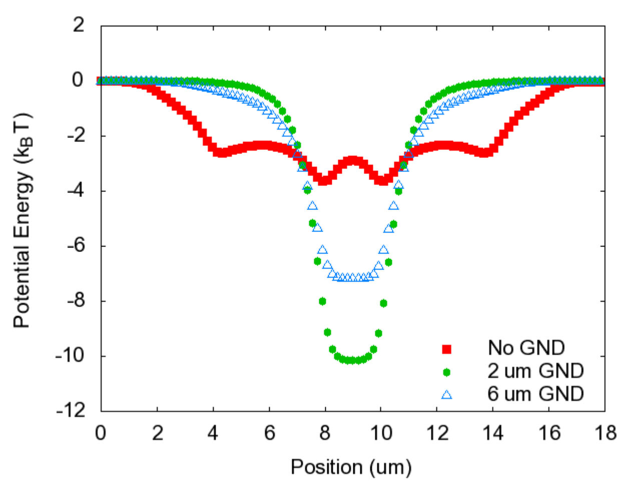

Figure 3: DEP potentials for one full period of electrodes. Active electrode is at 8-10 µm, inactive electrodes are at 2-4 and 14-16 µm. Cases with and without ground planes are shown.

Higher-phase rectification increases the length of the low-force region between wells. For certain potential well shapes and switching times, this can be beneficial because particles in the low-force regions are more likely to find their way to the leading well rather than the lagging well, which is now further away. If the separation is increased too much, particles spend more time in the low-force region before being caught in another well, effectively decreasing their net average velocity.

Our simulations show that four-phase rectification in the case of no ground plane offers a substantial improvement, with no additional gains from higher-phase schemes. However, for the more narrowly focused, deep potential wells resulting from the presence of a ground plane (Fig. 3), three-phase rectification is preferable. Placing the ground electrode immediately above the channel creates very strong coupling between the active electrode and the plane thereby creating a narrow potential well. Positioning the ground plane at a distance on the order of the inter-electrode spacing broadens the well, creating a larger capture region, which enhances transport, as shown in Fig. 6.

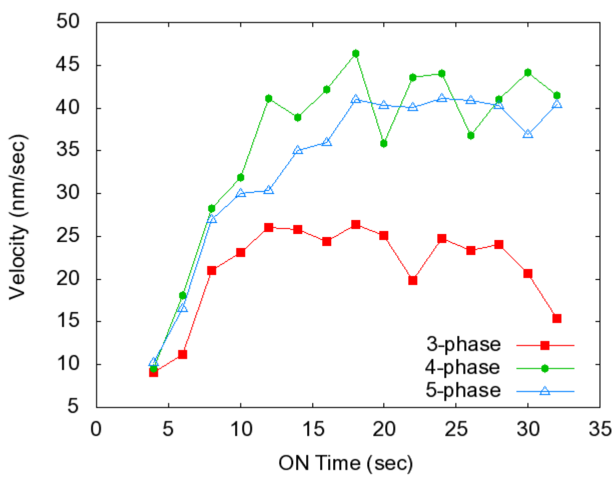

Figure 4: Average velocities for different rectification schemes with no ground plane. OFF time is 0 s and number of cycles is 5.

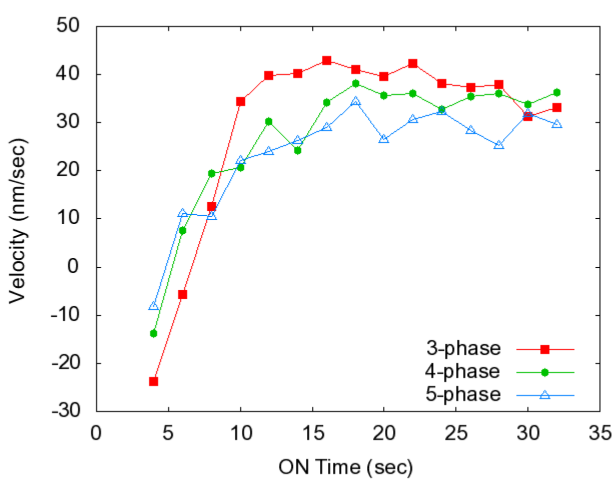

Figure 5: Average velocities for the system with ground plane directly above the channel.

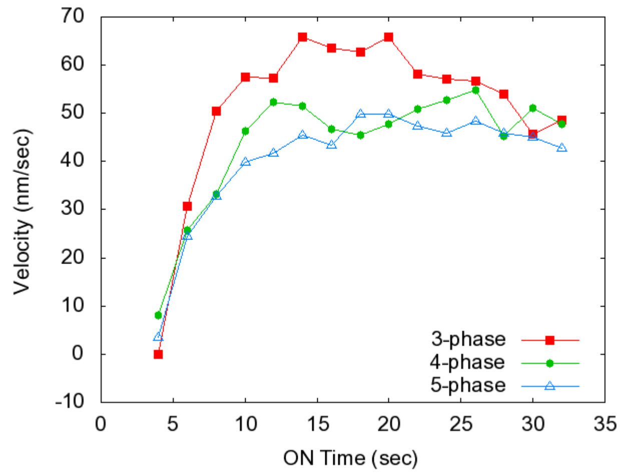

Figure 6: Average velocities for the system with ground plane 6 μm above the bottom of the channel.

Effect of Barrier on Transport

Systems lacking a ground plane, with electric field coupling between adjacent electrodes, may have a potential barrier located directly above the active electrode. Reducing the channel height to 1 μm, as fabricated in [3], produces exactly such a case. We have investigated the effect of this potential barrier by fitting the potential profile to an expression,

$$U(x) = -A \cdot \left(\exp\left\{ -\left[M \cdot \left(\frac{x-B}{C} \right)^2 \right]^N \right\} + \exp\left\{ -\left[M \cdot \left(\frac{x+B}{C} \right)^2 \right]^N \right\} \right)^{\frac{1}{M}} \quad (6)$$

where A, M, B, C, and N are fitting parameters, in order to easily perturb the barrier and observe the effect on transport. There is no physical basis for this expression; it is simply an *ad-hoc* functional form that closely matches the shape of the potentials obtained with electrostatic simulations. This potential profile is shown in Fig. 7 alongside cases with modified barrier height. Table 1 lists the fitting parameters used.

Table 1: Parameters used in Fig. 7 (k_B is Boltzmann's constant, T is temperature.)

	Fit	Small Barrier	Large Barrier
A (k_BT)	5.4	5.4	5.4
B (μm)	3.0	2.9	3.1
C (μm)	2.9	3.1	2.7
N	2.7	2.7	2.7
M	1.2	1.2	1.2

Fig. 8 shows the velocity curves for each case along with data from Altintas [3]. As before, the OFF time is 0 s and the number of cycles is fixed at 5. Three-phase rectification was used and motion along the y-axis was disabled. Reducing the barrier height is found to greatly enhance transport. This is because a reduced barrier makes it more likely that particles in either minimum can cross over to the other. When the profile is first moved forward 6 μm, the particles previously in the right half of the well find themselves in the left half. With the lower barrier, they are more likely to overcome the barrier into the right half again, effectively moving them forward and increasing their transport velocity.

We find that the experimental data most closely matches the small barrier potential rather than the one fit to COMSOL data. The performance of the Brownian motor in simulation is extremely sensitive to variations in the potential profile, which leads us to speculate that the fabricated system may differ from the 2D COMSOL simulation. There are many possible sources of inaccuracy: variations and deviations from specifications introduced during fabrication as well as the effect of the finite-width channels (necessitating fully 3D simulations).

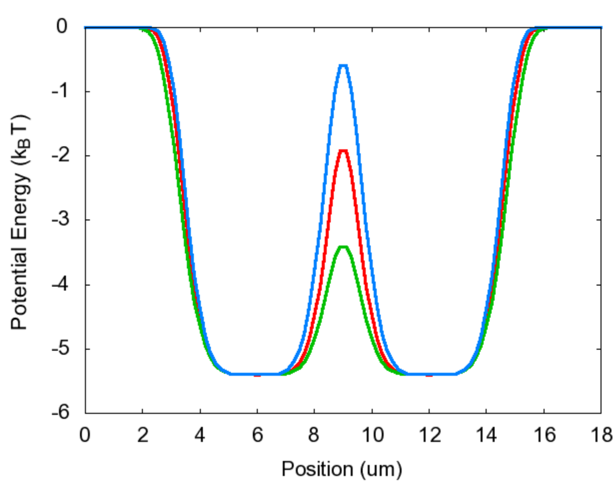

Figure 7: Functional potentials with different barrier heights. The center case is a close approximation of the potential profile calculated for a 1 μm channel system.

CONCLUSION

We have demonstrated a tool that has enabled us to identify strategies for improving the performance of the linear Brownian motor developed in Altintas *et al.* [2,3,7]. We show that modifying the rectification scheme alone can improve transport velocity by 73% (in the case of no ground plane) and additional gains can be achieved by positioning a ground plane above the channel. Deep potential wells with wide capture regions are desirable, and split wells with multiple minima and barriers are not. Depending on the shape of the potential profile, increasing the rectification scheme beyond three phases may enhance performance, a simple modification to perform because it requires no change to the physical structure of the device.

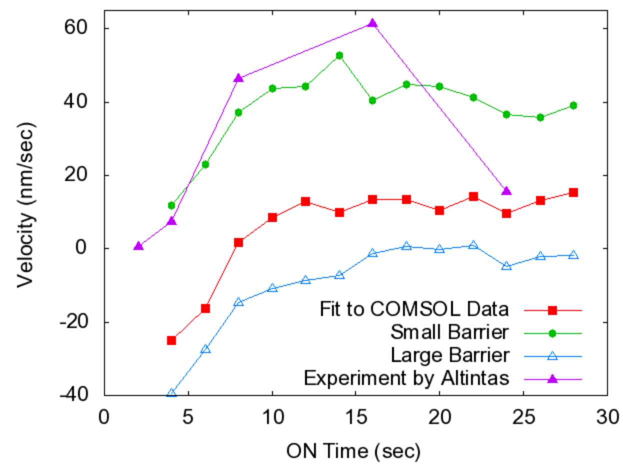

Figure 8: Velocity curves versus ON time for different barrier heights and comparison to data from Altintas [3].

REFERENCES

[1] P. Reimann, "Brownian motors: noisy transport far from equilibrium," *Phys. Reports*, vol. 361, pp. 57-265, 2001.

[2] E. Altintas, E. Sarajlic, K. Böhringer, H. Fujita, "Speed Performance and Control of Micromachined Linear Brownian Motor," *21st IEEE International Conference on Micro Electro Mechanical Systems (MEMS'08)*, Tucson, AZ, January 13-17, 2008.

[3] E. Altintas, "Micromachined Brownian Motors: Unidirectional Actuation of Nanoparticles by Rectified Brownian Motion," Ph.D. Thesis, Univ. of Tokyo, 2008.

[4] Ł. Machura, "Performance of Brownian Motors," Ph.D. Thesis, Univ. of Augsburg, 2006.

[5] M. Washizu, S. Suzuki, O. Kurosawa, T. Nishizaka, T. Shinohara, "Molecular Dielectrophoresis of Biopolymers," *IEEE Transactions on Industry Applications*, vol. 30, no. 4, 1994.

[6] A. Castellanos, A. Ramos, A. Gonzalez, N. Green, H. Morgan, "Electrohydrodynamics and dielectrophoresis in microsystems: scaling laws," *Journal of Physics D*, 36, pp. 2584-2597, 2003.

[7] E. Altintas, E. Sarajlic, K. Böhringer, H. Fujita, "Speed Performance and Control of Micromachined Linear Brownian Motor," *21st IEEE International Conference on Micro Electro Mechanical Systems (MEMS'08)*, Tucson, AZ, January 13-17, 2008.

CONTACT

* B.C. Trzynadlowski, trzy@u.washington.edu